

## THE CASIMIR EFFECT IN RELATIVISTIC QUANTUM FIELD THEORIES\*

V. M. MOSTEPANENKO<sup>†,‡</sup>

*Center of Theoretical Studies Institute for Theoretical Physics, Leipzig University,  
Augustusplatz 10/11, 04109, Leipzig, Germany*

<sup>‡</sup>*E-mail: Vladimir.Mostepanenko@itp.uni-leipzig.de*

We review recent developments in the Casimir effect which arises in quantization volumes restricted by material boundaries and in spaces with non-Euclidean topology. The starting point of our discussion is the novel exact solution for the electromagnetic Casimir force in the configuration of a cylinder above a plate. The related work for the scalar Casimir effect in sphere-plate configuration is also considered, and the application region of the proximity force theorem is discussed. Next we consider new experiments on the measurement of the Casimir force between metals and between metal and semiconductor. The complicated problem connected with the theory of the thermal Casimir force between real metals is analyzed in detail. The present situation regarding different theoretical approaches to the resolution of this problem is summarized. We conclude with new constraints on non-Newtonian gravity obtained using the results of latest Casimir force measurements and compare them with constraints following from the most recent gravitational experiments.

*Keywords:* Casimir effect; exact solutions; Nernst heat theorem; non-Newtonian gravity.

### 1. Introduction

The Casimir effect<sup>1</sup> is a particular type of vacuum polarization which arises in quantization volumes restricted by material boundaries and in spaces with non-Euclidean topology due to distortions in the spectrum of zero-point oscillations of relativistic quantized fields in comparison with the case of free infinite Euclidean space-time. In case of volumes restricted by material boundaries, the polarization energy results in the Casimir force acting on these boundaries. In spaces with non-Euclidean topology, the polarization stress-energy tensor influences the geometry of space-time through the Einstein equations of gravitational field. In both cases the applications of the Casimir effect are extraordinary wide and range from condensed matter physics, atomic physics and nanotechnology to gravitation and cosmology (see monographs 2–5 and reviews 6–8).

During the last few years the Casimir force was measured with increased precision in configurations metal-metal<sup>9–20</sup> and metal-semiconductor.<sup>21–23</sup> The theory of the Casimir effect was widened to incorporate real material properties<sup>7</sup> and more complicated geometrical configurations.<sup>24,25</sup> Much attention was given to the controversial problem of the thermal Casimir force between real metals (see discussion in Refs. 26,27) and dielectrics.<sup>28–30</sup> The results of precise measurements of the Casimir force between metal surfaces were used for obtaining stronger constraints

---

\*This research has been partially supported by DFG grant 436 RUS 113/789/0–2.

<sup>†</sup>On leave from Noncommercial Partnership “Scientific Instruments”, Tverskaya St. 11, Moscow, 103905, Russia.

on the Yukawa-type corrections to Newtonian gravitational law predicted in unified gauge theories, supersymmetry and supergravity.<sup>18–20,31</sup>

In the present paper we discuss the above most important achievements in the Casimir physics for the period after the Xth Marcel Grossmann Meeting which was hold in July, 2003 at Rio de Janeiro. In our opinion, the theoretical achievement of major significance during this period is the obtaining the exact solution for the electromagnetic Casimir force in configuration of a cylinder above a plate<sup>24</sup> (see also further development of this matter in Ref. 25). The related work was done for the scalar Casimir force in configurations of a sphere or a cylinder above a plate.<sup>25,32</sup> In Ref. 33 the scalar Casimir effect in the same configurations was considered numerically using the worldline algorithms. The combination of the exact analytical and precise numerical methods permitted to make some conclusions on the validity limits of the so-called proximity-force theorem (PFT) which is heavily used in the experimental investigation of the Casimir force. All these results are discussed in Sec. 2 of the present paper.

Sec. 3 is devoted to new experiments on the measurement of the Casimir force between metals<sup>18–20</sup> and between metal and semiconductor.<sup>21–23</sup> The experiments<sup>18–20</sup> using a micromechanical torsional oscillator permitted for the first time to achieve the recordly low total experimental error of about 0.5% within a wide separation range and reliably decide between different competing approaches to the theoretical description of the thermal Casimir force. The experiments<sup>21–23</sup> using an atomic force microscope opened new prospective opportunities for the control of the Casimir force in nanodevices by changing the charge carrier density in a semiconductor test body.

The complicated theoretical problems related to the thermal Casimir force are discussed in Sec. 4. As underlined in this section, the theoretical approach proposed by some authors for real metals<sup>27</sup> is not only in contradiction to experiment, but inavoidably results in a violation of the Nernst heat theorem.<sup>26,34,35</sup> What is more, we stress that the same problems, as for real metals, arise for the Casimir force in configurations of two dielectrics and metal-dielectric if dc conductivity of a dielectric plate is taken into account.<sup>28–30</sup> This suggests that there are serious restrictions in a literal application of the Lifshitz theory to real materials. Some phenomenological approaches on how to avoid contradictions with theormodynamics and experiment proposed in literature are discussed.

In Sec. 5 reader finds the review of new constraints on non-Newtonian gravity obtained from recent measurements of the Casimir force between metallic test bodies.<sup>18–20,31</sup> These constraints are compared with those obtained from gravitational measurements.

Sec. 6 contains our conclusions and discussions.

## 2. New exact solutions in configurations with curved boundaries

It is common knowledge that Casimir<sup>1</sup> found the exact expression

$$F(z) = -\frac{\pi^2}{240} \frac{\hbar c}{z^4} \quad (1)$$

for the fluctuation force of electromagnetic origin per unit area acting between two plane-parallel ideal metal plates at a separation  $z$ . Lifshitz theory<sup>36</sup> generalized Eq. (1) for the case of two parallel plates described by a frequency-dependent dielectric permittivity  $\varepsilon(\omega)$ . Experimentally it is hard to maintain the parallelity of the plates. Because of this, most of experiments were performed using the configuration of a sphere above a plate. The configuration of a cylinder above a plate also presents some advantages if to compare with the case of two parallel plates. Unfortunately, over many years it was not possible to obtain exact expressions for the Casimir force in these configurations. For this reason, the approximative proximity-force theorem<sup>37</sup> (PFT) was used to compare experiment with theory. According to the PFT, at short separations ( $z \ll R$ ) the Casimir forces between an ideal metal cylinder (per unit length) or a sphere and a plate are given by

$$F_c(z) = -\frac{\pi^3}{384\sqrt{2}} \sqrt{\frac{R}{z}} \frac{\hbar c}{z^3}, \quad F_s(z) = -\frac{\pi^3}{360} \frac{\hbar c R}{z^3}, \quad (2)$$

where  $R$  is a sphere or a cylinder radius.

Within the PFT it is not possible to control the error of the approximate expressions in Eq. (2). From dimensional considerations it was evident<sup>7</sup> that the relative error in Eq. (2) should be of order of  $z/R$ , but the numerical coefficient near this ratio remained unknown. In fact, rigorous determination of the error, introduced by the application of the PFT, requires a comparison of Eq. (2) with the exact analytical results or with precise numerical computations in respective configurations. One such result for the electromagnetic Casimir effect was first obtained<sup>24</sup> for a cylinder above a plate using a path-integral representation for the effective action. Eventually, the Casimir energy is expressed through the functional determinants of infinite matrices with elements given in terms of Bessel functions.<sup>24</sup> The analytic asymptotic behavior of the exact Casimir energy at short separations was found in Ref. 25. It results in the following expression for the Casimir force at  $z \ll R$ :

$$F_c(z) = -\frac{\pi^3}{384\sqrt{2}} \sqrt{\frac{R}{z}} \frac{\hbar c}{z^3} \left[ 1 - \frac{3}{5} \left( \frac{20}{3\pi^2} - \frac{7}{36} \right) \frac{z}{R} \right]. \quad (3)$$

Eq. (3) is of much importance. It demonstrates that the relative error of the electromagnetic Casimir force between a cylinder and a plate calculated using the PFT is equal to  $-0.288618z/R$ . Thus, for typical parameters of  $R = 100 \mu\text{m}$  and  $z = 100 \text{ nm}$  this error is approximately equal to only 0.03%.

For a sphere above a plate the analytic solution in the electromagnetic case is not yet obtained. The scalar Casimir energy for a sphere above a plate is found in Refs. 25 and 32. However, the asymptotic expression at short separations similar to Eq. (3) is not found. In Ref. 33 the scalar Casimir energies for both a sphere and

a cylinder above a plate are computed numerically using the worldline algorithms. It was supposed that a scalar field satisfies Dirichlet boundary conditions. As was noticed in Ref. 33, the Casimir energies for the Dirichlet scalar should not be taken as an estimate for those in electromagnetic case. In addition, it should be stressed that the errors of the PFT calculated in Ref. 33 are related to the Casimir energy and not to the experimentally measured Casimir force. This makes all errors larger. To illustrate, if we were considering the error of the PFT in application to the electromagnetic Casimir energy between a plate and a cylinder [instead of the force considered in Eq. (3)], the value of  $-0.48103z/R$  would be obtained as a negative error of the PFT.<sup>25</sup> The magnitude of the latter is by a factor of 1.6667 larger than the error obtained above for a force.

Eq. (3) confirms that PFT works well at short separations and reproduces the exact result with a very high precision. This justifies the use of the PFT for the interpretation of experimental data. In Refs. 38,39 it was claimed, however, that in the configurations of sinusoidally corrugated plates or a sphere above a plate the PFT overestimates the lateral Casimir force by up to 30–40%. Comment 40 demonstrates that these claims are not warranted. In Refs. 38,39 metal is described by the plasma model with a plasma wavelength  $\lambda_p = 136$  nm for Au. Deviations of the “exact” results obtained in Refs. 38,39 from those given by the PFT in plate-plate configuration are presented in Fig. 1 of Ref. 38 (Fig. 11 of Ref. 39) in terms of function  $\rho$  versus  $k = 2\pi/\lambda_C$ , where  $\lambda_C$  is the corrugation wavelength. According to this figure, the lateral force amplitude is less by 16% than the value given by the PFT for configuration with  $\lambda_C = 1.2$   $\mu\text{m}$  and plate separation  $z = 200$  nm (it is supposed that corrugation amplitudes are much less than  $z$ ,  $\lambda_p$  and  $\lambda_C$ ). This result of Refs. 38,39 is in contradiction with a more fundamental path-integral theory formulated for ideal metals.<sup>42</sup> It is easily seen, that the quantity  $\rho$ , plotted in the above-mentioned figures as a function of  $k$  at different  $z$  and with a fixed  $\lambda_p$ , is, in fact, a function of  $kz$ . Thus, for corrugated plates with rescaled  $\lambda_C = 12$   $\mu\text{m}$  and  $z = 2$   $\mu\text{m}$  (but with the same  $kz$ ) the deviation of the lateral force amplitude from the PFT value is still 16%. At  $z = 2$   $\mu\text{m}$ , however, the nonideality of a metal does not play any important role, and Ref. 42 demonstrates the complete agreement between the exact result and the PFT if (as it holds in our case)  $z$  is several times less than  $\lambda_C$ . Note that if the latter condition is not satisfied, the PFT underestimates the force amplitude,<sup>42</sup> and not overestimates it as in Refs. 38,39.

In the Reply<sup>41</sup> to the Comment<sup>40</sup> the authors of Refs. 39,40 claim that the above arguments raising doubts on their predictions are based on a mistake. This claim is in error. Reference 41 is right that generally the case of perfectly reflecting mirrors is recovered in the limit  $\lambda_p \rightarrow 0$ . In the formalism of Refs. 38,39, however, this limiting transition is forbidden by the condition that the corrugation amplitudes are much less than  $\lambda_p$ . Thus, for fixed corrugation amplitudes the limiting case of ideal metal cannot be achieved by decreasing  $\lambda_p$ . On the contrary, the formalism of Refs. 38,39 allows any increase of  $\lambda_C$  and  $z$ , and this was used in the Comment.<sup>40</sup> At separations  $z \gg \lambda_p$  (in the Comment  $z = 2$   $\mu\text{m}$ ) real metal behaves like ideal

metal and all results should coincide with those for ideal metals as obtained in the path-integral approach.<sup>42,43</sup> In fact, however, the results of Refs. 38,39 at large separations are drastically different from the results of Refs. 42,43 obtained for ideal metals. This leads us to the conclusion that the predictions of Refs. 38,39 made for the configuration of two corrugated plates are in error.

For the experimental configuration of a sphere above a plate Refs. 38,39 obtain the “exact” computational value 0.20 pN for the amplitude of the lateral force at a separation  $z = 221$  nm between the test bodies with corrugation amplitudes equal to  $A_1 = 59$  nm and  $A_2 = 8$  nm. According to Refs. 38,39, the linear in the corrugation amplitudes version of the PFT gives instead 0.28 pN, i.e., 40% difference. At this point Ref. 40 stresses that the amplitudes considered are not small comparing to  $z$  (for instance,  $A_1/z = 0.27$ ) and another assumption  $A_1, A_2 \ll \lambda_p$  used in Refs. 38,39 is also violated (for instance,  $A_1/\lambda_p = 0.43$ ). It is not surprising, then, that Refs. 38, 39 arrive at a force amplitude of 0.20 pN so far away from the value of 0.33 pN obtained theoretically using the complete PFT and that of  $0.32 \pm 0.077$  pN measured experimentally at 95% confidence in Ref. 17. Thus, the approach used in Refs. 38,39 is not only in contradiction with a more fundamental path-integral theory<sup>42</sup> but is also excluded by experiment.<sup>16</sup> This justifies the conclusion of Refs. 42,43 that the PFT presents correct description of the lateral Casimir force between corrugated test bodies when the separation is several times less than the corrugation period.

### 3. New precise measurements of the Casimir force between metal and semiconductor test bodies

The most important experiments on the Casimir force after the Xth Marcel Grossmann Meeting were performed at Purdue University — Indiana State University<sup>18–20</sup> and at the University of California, Riverside.<sup>21–23</sup> Two experiments in Refs. 18–20 are devoted to the determination of the Casimir pressure between two Au-coated plates using the dynamic techniques based on a micromechanical torsional oscillator. The improved version of this experiment is described in Refs. 19,20. The two test bodies of the micromechanical oscillator are a sphere and a plane plate. Sphere is oscillating with the angular resonant frequency, and the shift of this frequency under the influence of the Casimir force  $F$  acting between a sphere and a plate was measured as a function of separation  $z$  in the region from 160 to 750 nm. From this shift one can find<sup>15,18–20</sup> the force gradient  $\partial F/\partial z$  and using the PFT arrive to the equivalent Casimir pressure

$$P(z) = -\frac{1}{2\pi R} \frac{\partial F(z)}{\partial z}. \quad (4)$$

This experiment is characterized by a very low total experimental error which was determined at a 95% confidence level and varies between 0.55 and 0.60% in a wide separation region from 170 to 350 nm.

The obtained experimental results were compared with different theoretical approaches using the Lifshitz theory<sup>36</sup> and tabulated optical data for the complex

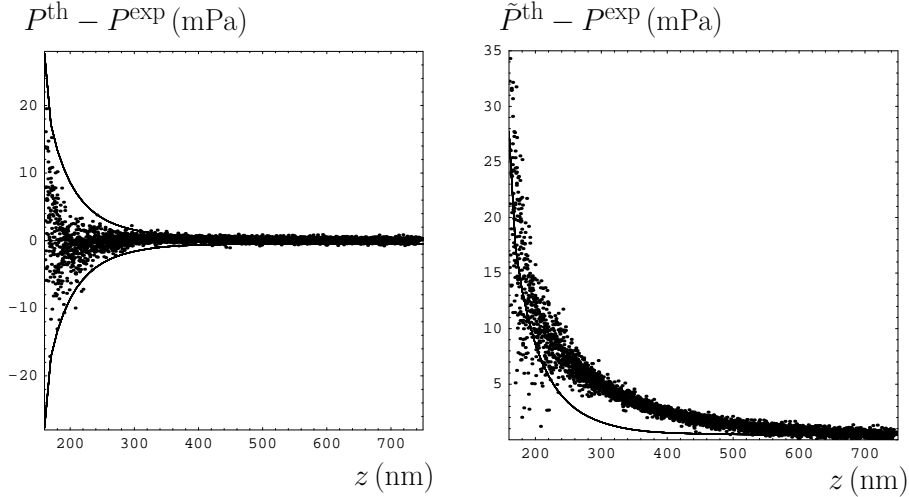


Fig. 1. Differences of the theoretical and experimental Casimir pressures versus separation (dots) and the 95% confidence intervals (solid lines). The theoretical pressures  $P^{\text{th}}$  (left figure) are computed using the impedance approach and  $\tilde{P}^{\text{th}}$  (right figure) using the Drude model approach.

index of refraction.<sup>44</sup> In this comparison all corrections due to surface roughness, nonzero temperature, sample-to-sample variations of optical data, errors of the PFT, effects of spatial nonlocality and of patch potentials were carefully analyzed and taken into account in a conservative way. Specifically, the error of the PFT was conservatively estimated as equal to  $z/R$ , whereas recent results presented in Sec. 2 lead to several times smaller error. It was concluded that data are consistent with the surface impedance approach to the thermal Casimir force at the laboratory temperature  $T = 300$  K (see Fig. 1, left, where the differences between theoretical,  $P^{\text{th}}$ , and experimental,  $P^{\text{exp}}$ , Casimir pressures are plotted versus separation). The data were found to be consistent also with the theoretical approach using the plasma model at  $T = 300$  K, and with the theoretical computations at zero temperature. At the same time, Fig. 1, right, shows that experimental data exclude theoretical Casimir pressures,  $\tilde{P}^{\text{th}}$ , computed using the Drude model approach at  $T = 300$  K (discussion of different theoretical approaches is contained in Sec. 4).

The experiment by using a micromechanical torsional oscillator has permitted also to obtain stronger constraints on non-Newtonian gravity which are considered in Sec. 5.

Three experiments in Refs. 21–23 are devoted to the measurement of the Casimir force acting between Au-coated sphere and single-crystal Si plates with different charge carrier densities using an atomic force microscope. In Ref. 21 B-doped Si plate with a resistivity  $\rho \approx 0.0035 \Omega \text{cm}$  and concentration of charge carriers  $n \approx 3 \times 10^{19} \text{cm}^{-3}$  was used. The measured force-distance relation of the Casimir force was compared with two theoretical dependences. One of them was computed for this sample and another one for a sample made of Si with high resistivity equal to  $1000 \Omega \text{cm}$ . It was found that theoretical results computed for the semiconductor

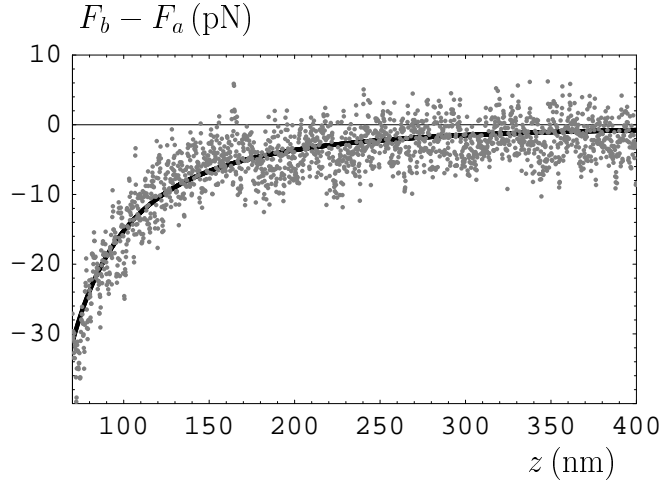


Fig. 2. The differences of the mean measured Casimir forces of the lower and higher resistivity Si (dots) and respective theoretical difference (solid line) versus separation

plate used in experiment are consistent with the data. At the same time, theoretical results computed for high-resistivity Si are experimentally excluded at 70% confidence. This suggests that the Casimir force is sensitive to the conductivity properties of semiconductors.

The obtained results were confirmed in the direct measurement of the difference Casimir force acting between Au-coated sphere and two P-doped Si plates of different charge carrier densities.<sup>22</sup> One of the silicon plates (sample *a*) had the resistivity  $\rho_a \approx 0.43 \Omega \text{ cm}$  and the concentration of charge carriers  $n_a \approx 1.2 \times 10^{16} \text{ cm}^{-3}$ . Another one (sample *b*) had much lower resistivity  $\rho_b \approx 6.4 \times 10^{-4} \Omega \text{ cm}$  and much higher concentration of charge carriers  $n_b \approx 3.2 \times 10^{20} \text{ cm}^{-3}$ . In Fig. 2, taken from Ref. 22, the difference of experimental mean Casimir forces, acting between Au-coated sphere and samples *b* and *a*,  $F_b - F_a$ , versus separation is shown as dots. The theoretically calculated differences using the Lifshitz formula are shown by the solid line. Within the separations from 70 to 100 nm the mean difference in the measured Casimir forces exceeds the experimental error of force difference. This permits a conclusion that in Ref. 22 the influence of charge carrier density of a semiconductor on the Casimir force was experimentally measured for the first time.

The third experiment on the measurement of the Casimir force between Au-coated sphere and single-crystal Si plate demonstrates a new physical phenomenon, the modulation of the Casimir force with laser light.<sup>23</sup> In the absence of light the used Si plate had a relatively high resistivity  $\rho \approx 10 \Omega \text{ cm}$  and relatively low concentration of charge carriers  $n \approx 5 \times 10^{14} \text{ cm}^{-3}$ . This plate was illuminated with 514 nm pulses, obtained from an Ar laser. In the presence of pulse the concentration of charge carriers increases up to  $n \approx 2 \times 10^{19} \text{ cm}^{-3}$ . The difference of the Casimir forces in the presence and in the absence of pulse,  $\Delta F$ , was measured using

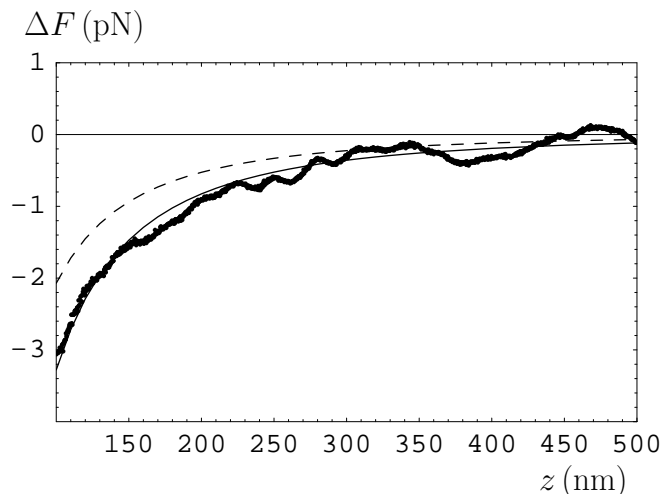


Fig. 3. The differences of the mean measured Casimir forces with laser pulse on and off (dots) versus separation. The respective theoretical differences are computed under the assumption of finite static dielectric permittivity of Si in the absence of laser light (solid line) and taking dc conductivity of high-resistivity Si into account (dashed line).

an atomic force microscope within the separation range from 100 to 500 nm. The experimental results<sup>23</sup> are shown in Fig. 3 as dots versus separation. In the same figure the solid line is computed using the Lifshitz formula under the assumption that in the absence of laser light Si possesses a finite static dielectric permittivity  $\epsilon^{Si}(0) = 11.66$ . The dashed line is computed taking into account the dc conductivity of Si in the absence of laser light at frequencies much below the first Matsubara frequency. As is seen in Fig. 3, the solid line is in excellent agreement with the experimental data, whereas the dashed line is in disagreement with data. Physical consequences following from this observation are discussed in the next section.

The demonstrated dependence of the Casimir force between a metal and a semiconductor on the density of charge carriers in semiconductor can be applied in nanodevices of the next generations such as micromirrors, nanotweezers and nanoscale actuators. In so doing, the density of charge carriers can be changed either by doping and/or due to irradiation of a device by laser light leading to respective variations in the magnitude of the Casimir force.

Since the Xth Marcel Grossmann Meeting in 2003, some other experiments on the Casimir force have been proposed. One could mention the proposal to measure the influence of the Casimir energy on the value of the critical magnetic field in superconductor phase transitions,<sup>45</sup> the suggestion to measure the Casimir torques using the repulsive force due to liquid layers,<sup>46</sup> and the proposed Casimir force measurements at large separations.<sup>47–49</sup> Special attention was attracted to new techniques for the measurement of the Casimir force. Thus, in Ref. 50 the holographic



interferometer was first applied for optical detection of mechanical deformation of a macroscopic object induced by the Casimir force. All this demonstrates that there are considerable opportunities in the experimental investigation of the Casimir force and in applications of the Casimir effect.

#### 4. Problems in the theory of thermal Casimir force between metals and dielectrics

During all the period between the Xth and XIth Marcel Grossmann Meetings the problem of the thermal Casimir force was hotly debated. Until 2005, only the case of two plates made of real metal was the subject of controversy. In 2005 it was shown, however, that the case of two dielectric plates leads to problems as well.<sup>28</sup>

We start from the Lifshitz formula for the free energy of the van der Waals (Casimir) interaction between two semispaces with a gap of width  $z$  in thermal equilibrium at temperature  $T$ :

$$\mathcal{F}(z, T) = \frac{k_B T}{2\pi} \sum_{l=0}^{\infty} \left(1 - \frac{1}{2} \delta_{l0}\right) \int_0^{\infty} k_{\perp} dk_{\perp} \quad (5)$$

$$\times \left\{ \ln [1 - r_{\text{TM}}^2(\xi_l, k_{\perp}) e^{-2q_l z}] + \ln [1 - r_{\text{TE}}^2(\xi_l, k_{\perp}) e^{-2q_l z}] \right\}.$$

Here  $k_B$  is the Boltzmann constant,  $\xi_l = 2\pi k_B T l / \hbar$  are the Matsubara frequencies,  $q_l = (k_{\perp}^2 + \xi_l^2 / c^2)^{1/2}$ ,  $k_{\perp}$  is the projection of the wave vector on the boundary planes of semispaces, and  $r_{\text{TM,TE}}(\xi_l, k_{\perp})$  are the reflection coefficients for two independent polarizations of the electromagnetic field (transverse magnetic and transverse electric modes).

In the original formulation of the Lifshitz theory the semispace material is described by using the approximation of dielectric permittivity  $\varepsilon(\omega)$  depending only on the frequency, and the continuity conditions

$$E_{1t} = E_{2t}, \quad B_{1t} = B_{2t}, \quad D_{1n} = D_{2n}, \quad B_{1n} = B_{2n} \quad (6)$$

for the electric field, magnetic induction and electric displacement on boundary planes. Thus, the Lifshitz theory does not take into account the effects of spatial dispersion. In this model case the reflection coefficients take the form

$$r_{\text{TM}}(\xi_l, k_{\perp}) = \frac{\varepsilon_l q_l - k_l}{\varepsilon_l q_l + k_l}, \quad r_{\text{TE}}(\xi_l, k_{\perp}) = \frac{k_l - q_l}{k_l + q_l}, \quad (7)$$

where  $k_l = \sqrt{k_{\perp}^2 + \varepsilon_l \xi_l^2 / c^2}$  and  $\varepsilon_l = \varepsilon(i\xi_l)$ .

The central point of the debates is the term of Eq. (5) with  $l = 0$  (the so-called zero-frequency term). At large separations (high temperatures) it is dominant, and all terms with  $l \geq 1$  are negligibly small independently of the specific form of  $\varepsilon(\omega)$ . The case of ideal metal plates is obtained from Eqs. (5), (7) using the so-called Schwinger prescription,<sup>5,51</sup> i.e., that one should take limit  $\varepsilon \rightarrow \infty$  first and set  $l = 0$  afterwards. Using this prescription, for ideal metal plates one obtains

$$r_{\text{TM}}(0, k_{\perp}) = 1, \quad r_{\text{TE}}(0, k_{\perp}) = 1. \quad (8)$$

The same result follows for ideal metal independently of the Lifshitz formula from thermal quantum field theory with boundary conditions in the Matsubara formulation. Thus, at large separations (in fact at separations larger than  $6 \mu\text{m}$  at  $T = 300 \text{ K}$ ) it follows

$$\mathcal{F}(z, T) = -\frac{k_B T}{8\pi z^2} \zeta(3), \quad (9)$$

where  $\zeta(3)$  is the Riemann zeta function. Notice that Eq. (9) is in agreement with the classical limit based on the Kirchoff's law.<sup>52,53</sup>

Refs. 54–57 (see also Ref. 27) suggested to calculate the thermal Casimir force by describing the properties of real metals at low frequencies via the dielectric permittivity of the Drude model

$$\varepsilon(i\xi) = 1 + \frac{\omega_p^2}{\xi [\xi + \gamma(T)]}, \quad (10)$$

where  $\omega_p$  is the plasma frequency and  $\gamma(T)$  is the relaxation parameter. Substituting Eq. (10) in Eq. (7) we obtain

$$r_{\text{TM}}(0, k_\perp) = 1, \quad r_{\text{TE}}(0, k_\perp) = 0. \quad (11)$$

Eq. (11) is preserved also in the limit of ideal metal plates, and is thus in contradiction with Eq. (8). From Eqs. (5) and (11) at large separations one arrives at the result

$$\mathcal{F}(z, T) = -\frac{k_B T}{16\pi z^2} \zeta(3) \quad (12)$$

instead of Eq. (9). This result is in contradiction with the classical limit.

Real metals in the frequency region of infrared optics are well described by the dielectric permittivity of the plasma model

$$\varepsilon(i\xi) = 1 + \frac{\omega_p^2}{\xi^2}. \quad (13)$$

If one extrapolates this model to low frequencies, the reflection coefficients become<sup>58,59</sup>

$$r_{\text{TM}}(0, k_\perp) = 1, \quad r_{\text{TE}}(0, k_\perp) = \frac{\sqrt{c^2 k_\perp^2 + \omega_p^2} - k_\perp}{\sqrt{c^2 k_\perp^2 + \omega_p^2} + k_\perp}. \quad (14)$$

In the limiting case of ideal metal plates it holds  $\omega_p \rightarrow \infty$  and Eq. (14) agrees with Eq. (8) because  $r_{\text{TE}}(0, k_\perp) \rightarrow 1$ . At large separations the plasma model leads to Eq. (9) in agreement with the classical limit.

It is notable that the plasma model predicts small thermal corrections to the Casimir force at short separations in qualitative agreement with the case of ideal metals (a fraction of a percent at separations below  $1 \mu\text{m}$ ). Much larger thermal corrections at short separations are predicted by using the Drude model (19% of the force at  $z = 1 \mu\text{m}$ ).

As was mentioned above, the dielectric permittivity depending on the frequency provides only an approximative description of metals because it disregards the effects of spatial dispersion. Another approximative description of metals is provided by the Leontovich impedance boundary condition

$$\mathbf{E}_t = Z(\omega) [\mathbf{B}_t \times \mathbf{n}], \quad (15)$$

where the index  $t$  labels the field components tangential to the plates,  $\mathbf{n}$  is the unit vector directed into the medium, and impedance function  $Z(\omega)$  is found from the solution of kinetic equations.<sup>60</sup> It is notable that the Leontovich impedance is well defined even in some frequency regions (for example, in the region of the anomalous skin effect in which the spatial dispersion is present) where the description in terms of  $\varepsilon(\omega)$  is not possible. At the same time, the Leontovich impedance is not applicable at separations  $z < \lambda_p = 2\pi c/\omega_p$ , where the inequality  $Z \ll 1$  may be violated and the boundary condition (15) cannot be used. In the frequency regions where both quantities are well defined it holds  $Z(\omega) = 1/\sqrt{\varepsilon(\omega)}$ .

In terms of Leontovich impedance, the reflection coefficients in the Lifshitz formula take the form<sup>61,62</sup>

$$r_{\text{TM}}(0, k_\perp) = \frac{cq_l - Z_l \xi_l}{cq_l + Z_l \xi_l}, \quad r_{\text{TE}}(0, k_\perp) = \frac{\xi_l - cq_l Z_l}{\xi_l + cq_l Z_l}, \quad (16)$$

where  $Z_l = Z(i\xi_l)$ . The zero-frequency values of these reflection coefficients depend on the form of impedance function used. For the impedance function of the normal and anomalous skin effect,<sup>60</sup> one reobtains Eq. (8) obtained previously for ideal metals. For the impedance function of the infrared optics it follows that

$$r_{\text{TM}}(0, k_\perp) = 1, \quad r_{\text{TE}}(0, k_\perp) = \frac{\omega_p - ck_\perp}{\omega_p + ck_\perp}. \quad (17)$$

In the limit of ideal metal plates  $\omega_p \rightarrow \infty$  and Eq. (17) coincides with Eq. (8). The Leontovich impedance leads to almost the same results for the thermal Casimir force as the plasma model, i.e., to small thermal corrections to the zero-temperature force at short separations and to Eq. (9) at large separations.

From the above it is seen, that there are three theoretical approaches using the Drude model, the plasma model and the Leontovich impedance which lead to different predictions for the thermal Casimir force. There is also the similarity between the plasma model approach and the impedance approach which both predict small thermal effects at short separations and are in agreement with the classical limit at large separations. This is in opposition to the Drude model approach which predicts relatively large thermal effect at short separations and is in violation of the classical limit at large separations.

As was analytically proved in Refs. 63,64 (see also Refs. 26,35), the Drude model approach leads to a violation of the third law of thermodynamics (the Nernst heat theorem) in the case of metallic perfect lattices with no defects and impurities. For such lattices the relaxation parameter  $\gamma(T) \rightarrow 0$  when  $T \rightarrow 0$  in accordance with

the Bloch-Grüneisen law and the entropy of a fluctuating field at zero temperature takes a negative value<sup>26,35,64</sup>

$$S(z, 0) = \frac{k_B}{16\pi z^2} \int_0^\infty y dy \ln \left[ 1 - \left( \frac{cy - \sqrt{4z^2\omega_p^2 + c^2y^2}}{cy + \sqrt{4z^2\omega_p^2 + c^2y^2}} \right)^2 e^{-y} \right] < 0, \quad (18)$$

instead of zero as is demanded by the Nernst heat theorem. At large separations from Eq. (18) it follows

$$S(z, 0) = -\frac{k_B\zeta(3)}{16\pi z^2} < 0, \quad (19)$$

i.e., what is called in Refs. 27,55–57 the entropy of a “modified ideal metal” (MIM) at zero temperature. Recent Refs. 27,57 recognize that their MIM violates the Nernst heat theorem but argue<sup>27</sup> that “the crucial difference between real metals and MIM is that the former includes relaxation by which there will be no violation of the third law of thermodynamics”. This conclusion is wrong because Eq. (18) proves the violation of the Nernst heat theorem for Drude metals with dielectric permittivity (10). These metals have a finite permittivity at all frequencies with exception of zero frequency and a nonzero relaxation described by the relaxation parameter  $\gamma(T)$ . From this it follows that the Drude model approach violates the third law of thermodynamics for perfect metallic crystal lattices with no impurities but nonzero relaxation at any nonzero temperature. Thus, theoretically this approach is not acceptable.

Several attempts were made to avoid this conclusion. In Refs. 56,65 the Drude model approach was applied to metallic lattices with defects and impurities possessing some residual relaxation  $\gamma(0) \neq 0$ . As a result, the equality  $S(z, 0) = 0$  was obtained which is in accordance with the Nernst heat theorem. This, however, does not solve the problem of the thermodynamic inconsistency of the Drude model approach, because metallic perfect crystal lattice with no impurities has a nondegenerate dynamic state of lowest energy. Thus, according to quantum statistical physics, the entropy at  $T = 0$  must be equal to zero for such crystal lattices [a property violated by the Drude model approach according to Eq. (18)].

Another attempt<sup>66</sup> includes spatial dispersion in the calculations of the Casimir energy. At large separations it arrives at the same Eq. (12) as was obtained by using the Drude model. At arbitrary separations between the plates computations in Ref. 66 nearly exactly coincide with earlier computations<sup>54</sup> using the Drude model. In Refs. 30,35,67 it was demonstrated, however, that the results of Ref. 66 are not reliable because the used approximative description of a spatial dispersion is unjustified. The main mistake in Ref. 66 is that it uses the standard continuity boundary conditions (6) on the electromagnetic field which are valid only in the absence of spatial dispersion. If the spatial dispersion is present, one must use instead the more complicated conditions<sup>68</sup>

$$E_{1t} = E_{2t}, \quad B_{1n} = B_{2n}, \quad D_{2n} - D_{1n} = 4\pi\sigma, \quad [\mathbf{n} \times (\mathbf{B}_2 - \mathbf{B}_1)] = \frac{4\pi}{c} \mathbf{j}, \quad (20)$$

where the induced charge and current densities are given by

$$\sigma = \frac{1}{4\pi} \int_1^2 \operatorname{div} [\mathbf{n} \times [\mathbf{D} \times \mathbf{n}]] dl, \quad \mathbf{j} = \frac{1}{4\pi} \int_1^2 \frac{\partial \mathbf{D}}{\partial t} dl. \quad (21)$$

In the Reply<sup>69</sup> to the Comment<sup>67</sup> the author attempts to avoid this conclusion by introducing the auxiliary fields and by bringing the Maxwell equations to the form with no induced charge and current densities. This attempt, however, fails because, as the author himself recognizes, the relations used by him are valid only in the Fourier space. In the case of temporal dispersion there is no problem in making the Fourier transform. However, for spatial dispersion in the presence of boundaries and a macroscopic gap between the two plates, this is not allowed.<sup>67</sup> The system under consideration in the Casimir effect is not spatially uniform and it is not possible to introduce the dielectric permittivity  $\varepsilon(\mathbf{q}, \omega)$  depending on both the wave vector and the frequency as is done in Refs. 66,69.

Reply<sup>69</sup> denies the note in the Comment<sup>67</sup> that the formalism used in the original work<sup>66</sup> involves nonconservation of energy. In support of this denial, it is argued that the energy leaving a region through an interface is entering the region on the other side, and, thus, energy is fully conserved. To arrive at this conclusion, the author admits that the in-plane components of the fields are continuous across the interface. In the presence of spatial dispersion this assumption is, however, not valid, as was demonstrated above. We underline that the violation of energy conservation in the so-called “dielectric approximation” of nonlocal electrodynamics used in Refs. 66,69 has long been rigorously proved<sup>70</sup> and discussed in the literature.<sup>68</sup>

To conclude, presently there is no question that the approach to the thermal Casimir force using the Drude model is thermodynamically invalid. At the same time, the plasma model and impedance approaches are consistent with thermodynamics. In particular, they satisfy the Nernst heat theorem.<sup>26,35</sup> In Refs. 28–30 it was shown that the same problems, as for metals, arise for dielectrics if one describes their conductivity at zero frequency with the help of the Drude model. This problem is more detailly discussed in another contribution to these Proceedings.<sup>71</sup>

Important problem is the comparison of different theoretical approaches to the thermal Casimir force with experiment. As was already emphasized in Sec. 3, the computations at zero temperature, and also theoretical approaches using the plasma model and the Leontovich surface impedance at  $T = 300$  K, are consistent with experiment (see, for example, Fig. 1, left). At the same time, the theoretical approach using the Drude model is excluded by experiment at 95% confidence level within the separation region from 170 to 700 nm. In the separation region from 300 to 500 nm the Drude model approach is excluded by experiment at even higher 99% confidence level.<sup>19,20</sup> For the purposes of comparison between experiment and theory, the computations of the Casimir pressure were done by using the tabulated optical data for the complex index of refraction<sup>44</sup> extended to lower frequencies. In fact, a marked difference between approaches arises only when calculating the con-

tribution of the zero-frequency term in the Lifshitz formula which should be found theoretically because at very low frequencies optical data are not available.

The comparison between experiment and theory in Fig. 1 is quite transparent. However, in Refs. 27,57 several objections against it were raised. According to Ref. 57, Purdue group<sup>18,19</sup> claims “the extraordinary high precision to be able to see our effect at distance as small as 100 nm” and “the accuracy is claimed to be better than 1% at separations down to less than 100 nm”. These statements are misleading because the experimental ranges in Refs. 18 and 19 are from 260 to 1100 nm and from 160 to 750 nm, respectively. There are no statements concerning the separations of 100 nm and below 100 nm in Refs. 18,19. According to another claim in Refs. 27,57, the determination of the absolute sphere-plate separation with the absolute error  $\Delta z = 0.6$  nm, as stated in Ref. 19, is difficult because “the roughness of the surfaces is much larger than the precision stated in the determination of the separation”. This claim is not right because the separations are measured between zero levels of the surface roughness. These zero levels are uniquely determined for any value of the roughness amplitude. One more claim<sup>57</sup> is that “the effects of surface plasmons<sup>72,73</sup> have not been included”. This claim is wrong because the computations in Refs. 18,19 were performed using the Lifshitz formula which includes in full the effects of surface plasmons.

As was noticed recently,<sup>74</sup> the precise values of the Drude parameters are important for an accurate calculation of the Casimir force in experimental configurations. According to Ref. 74, the use of different Drude parameters measured and calculated for different Au samples may lead to up to 5% variations in the magnitude of the Casimir force. In the computations of Refs. 18–20 the values  $\omega_p = 9.0$  eV and  $\gamma(T = 300 \text{ K}) = 0.035$  eV were used which are based on the experimental data of Ref. 44 and computations of Ref. 75. As was demonstrated above, these values lead to a very good agreement with traditional approaches to the thermal Casimir force which predict only small thermal corrections at short separations and exclude the Drude model approach. If much smaller value for Au plasma frequency were used in computations (i.e.,  $\omega_p = 6.85$  eV or 7.50 eV as suggested in Ref. 74) the agreement between the traditional theoretical approaches and experimental data would be worse for a few percent. The same holds for many other experiments on the Casimir effect.<sup>13,14,17–23</sup> It should be particularly emphasized that with smaller values of  $\omega_p$  the disagreement between the experimental data and the Drude model approach to the thermal Casimir force becomes much larger than is demonstrated in Fig. 1 (right). If one uses widely accepted criteria from the statistical theory of the verification of alternative hypotheses,<sup>76</sup> the hypothesis on much smaller magnitude of  $\omega_p$  (than that used in Refs. 18–20) is rejected at high confidence by all already performed experiments on the Casimir force with Au surfaces. This conclusion was recently confirmed<sup>77</sup> by the determination of the plasma frequency of Au coatings in the experimental configurations of Refs. 18–20 using the measured temperature dependence of the films resistivity. The obtained result  $\omega_p = 8.9$  eV [and a respective value for  $\gamma(T = 300 \text{ K}) = 0.0357$  eV] is in excellent agreement with Refs. 44,75.

It leads to even better than in Fig. 1 agreement of data with the traditional approaches to the thermal Casimir force and excludes the Drude model approach at the impressive 99.9% confidence level within a wide separation range. Thus, to date, it is beyond question that the Drude model approach is experimentally excluded.

One more important physical phenomenon which sheds light on the problem of the thermal Casimir force is the modulation of the Casimir force with laser light discussed in Sec. 3. From Fig. 3 it follows that the experimental data are consistent with theory if the dc conductivity of high resistivity Si in the absence of laser light is discounted. On the contrary, the dashed line takes into account dc conductivity of a Si plate in the absence of laser light described using the Drude dielectric function. As is seen in Fig. 3, the dashed line is experimentally excluded. Thus, for both metals and semiconductors the account of actual dielectric response at very low frequencies leads to contradictions between the Lifshitz theory and the experiment. To achieve an agreement between experiment and theory, one should use the dielectric response in the region of characteristic frequency  $\sim c/(2z)$  and extrapolate it to zero frequency. The complete understanding of this problem goes beyond the scope of the Lifshitz theory.

## 5. Constraints on new physics beyond the Standard Model

Many extensions of the Standard Model predict a new (so-called “fifth”) force co-existing with the usual Newtonian gravitational force and other conventional interactions. Such force can arise from the exchange of light elementary particles (e.g., scalar axions, graviphotons, dilatons, and moduli<sup>78,79</sup>), and as a consequence of extra-dimensional theories with low energy compactification scales.<sup>80,81</sup> The interaction potential of the fifth force acting between two point masses  $m_1$  and  $m_2$  at a distance  $r$  is conventionally represented as a Yukawa correction to the usual Newtonian potential

$$V(r) = -\frac{Gm_1m_2}{r} \left(1 + \alpha e^{-r/\lambda}\right), \quad (22)$$

where  $G$  is the gravitational constant,  $\alpha$  is a dimensionless constant characterizing the strength of the Yukawa force, and  $\lambda$  is its interaction range.

It has been known<sup>18–20,31,82–85</sup> that the best constraints on the parameters  $(\alpha, \lambda)$  in submicron range follow from the measurements of the Casimir force. The pressure of a hypothetical interaction,  $P^{\text{hyp}}(z)$ , which may act between experimental test bodies is computed<sup>18–20</sup> by the pairwise summation of potentials (22) with a subsequent negative differentiation with respect to separation. Then constraints on the hypothetical Yukawa-type pressure are found from the agreement between measurements and theory at 95% confidence level. According to the experimental results in Refs. 19,20, no deviations from calculations using the traditional theories of the Casimir force were observed. Thus, one can conclude that the hypothetical pressure should be less than or equal to the half-width of the confidence interval

$$|P^{\text{hyp}}(z)| \leq \Delta^{\text{tot}} [P^{\text{th}}(z) - P^{\text{exp}}(z)], \quad (23)$$

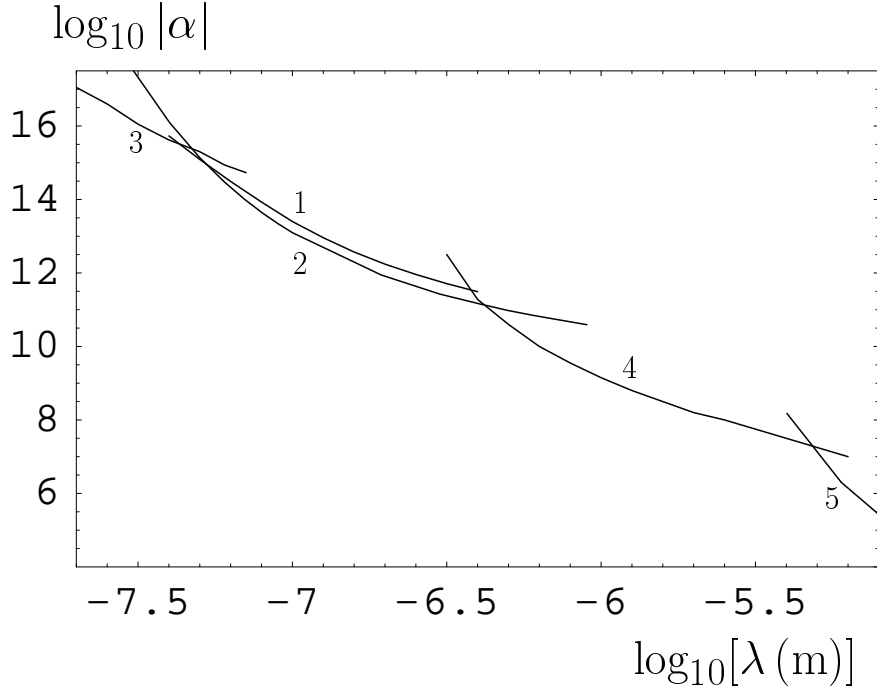


Fig. 4. Constraints on the Yukawa interaction constant  $\alpha$  versus interaction range  $\lambda$ . Line 1 is obtained from the measurements of the Casimir pressure by use of a micromechanical torsional oscillator.<sup>19,20</sup> Line 2 follows from the isoelectronic differential force measurements.<sup>31</sup> Line 3 is obtained from the measurement of the Casimir force using an atomic force microscope,<sup>13</sup> and line 4 from the torsion-pendulum experiment.<sup>9</sup> The strongest constraints following from the gravitational measurements using a micromachined cantilever<sup>86</sup> are indicated by the line 5.

where  $\Delta^{\text{tot}} [P^{\text{th}}(z) - P^{\text{exp}}(z)]$  is the total absolute error of the quantity  $P^{\text{th}}(z) - P^{\text{exp}}(z)$ . Note that just this error (and negative this error) are plotted in Fig. 1 (left and right) by the solid lines.

In Fig. 4 we plot the strongest constraints on  $\alpha$  for different values of  $\lambda$  following from the measurements of the Casimir force and compare them with the best gravitational experiments. Each line in Fig. 4 is related to some specific experiment. The region of  $(\alpha, \lambda)$  plane above each line is prohibited from the respective experiment and below each line is permitted. Constraints shown by line 1 follow from the most recent measurement of the Casimir pressure using a micromechanical torsional oscillator.<sup>19,20</sup> Line 3 is obtained<sup>85</sup> from the Casimir force measurement between an Au-coated sphere and a plate by means of an atomic force microscope.<sup>13</sup> Line 4 follows<sup>82</sup> from the measurement of the Casimir force between an Au-coated spherical lens and a plate by means of torsion pendulum.<sup>9</sup> Line 2 presents the constraints obtained from the first isoelectronic differential force measurement<sup>31</sup> between an Au-coated probe and two Au-coated films, made out of gold and germanium. In



this measurement the Casimir background is experimentally subtracted, thus avoiding the necessity to model the Casimir force. Finally, line 5 shows the most strong constraints on Yukawa-type deviations from Newtonian gravity obtained<sup>86</sup> from the gravitational experiment using a micromachined silicon cantilever as the force sensor at separations of order  $25\ \mu\text{m}$ , where the Casimir force is already negligibly small. Gravitational experiments provide also the strongest constraints on  $\alpha$  in the interaction range  $\lambda > 10^{-5}\ \text{m}$  (see Refs. 20,78 and 87 for more details).

As is seen in Fig. 4, at and below a micrometer interaction range there is no competitors to the Casimir effect in obtaining constraints on non-Newtonian gravity. During the last few years these constraints were strengthened by up to  $10^4$  times basing on the results of different measurements of the Casimir force between metal surfaces. Nevertheless, existing limits on  $\alpha$  below a micrometer are still relatively weak and should be strengthened by several orders of magnitude to reach the theoretically predicted regions of strange and gluon modulus, and of gauged barions.

## 6. Conclusions and discussion

In the foregoing, we have discussed main achievements in the physics of the Casimir effect during the period after the Xth Marcel Grossmann Meeting hold in 2003. In our opinion, the major theoretical breakthrough is the obtaining of the exact analytical solution for the electromagnetic Casimir energy in the configuration of an ideal metal cylinder above a plate. The resolution of this problem opened new opportunities for the investigation of the Casimir force between curved boundaries and permitted find first indisputable result on the accuracy of the PFT.

The major experimental breakthroughs during this period are the most precise measurements of the Casimir pressure between metal surfaces using a micromechanical oscillator (Decca et al.) and the first experiments on the Casimir effect in configuration of metal sphere and semiconductor plate by means of an atomic force microscope (Mohideen et al.). Both sets of experiments resulted in far-reaching and important conclusions. Experiments by Decca et al. have conclusively excluded large thermal corrections to the Casimir force at short separations as predicted by the Drude model approach. Experiments by Mohideen et al. demonstrated the possibility to control the Casimir force by changing the density of free charge carriers and led to new knowledge on the applicability of the Lifshitz theory to dielectrics.

Time between Xth and XIth Marcel Grossmann Meetings was marked by controversial discussions of different approaches to the theoretical description of the thermal Casimir force. During these discussions it was clearly demonstrated that all the proposed approaches are of approximate phenomenological character. None of them can yet claim to be the final fundamental resolution of the problem. Till the end of this period it was conclusively demonstrated that the Drude model approach is in contradiction with the foundations of thermodynamics and is excluded experimentally at a 99.9% confidence level. Important theoretical problem for future is

the fundamental understanding of the thermal Casimir force and related physical phenomena caused by vacuum and thermal oscillations of the electromagnetic field (e.g., atomic friction, radiative heat transfer etc.). The experimental challenge for near future is the measurement of the thermal effect in the Casimir force which has not been measured yet.

Both recent theoretical achievements and the performed experiments confirm the unique potential of the Casimir effect both in fundamental physics for constraining predictions of new unification physical theories beyond the Standard Model and in nanotechnology for fabrication, operation and control of a new generation of microdevices. This confirms the increasing role of the Casimir effect both in modern physics and in technological applications.

### Acknowledgments

The author is grateful for helpful discussions with M. Bordag, R. S. Decca, E. Fischbach, B. Geyer, G. L. Klimchitskaya, D. E. Krause, and U. Mohideen.

### References

1. H. B. G. Casimir, *Proc. K. Ned. Akad. Wet.* **51**, 793 (1948).
2. P. W. Milonni, *The Quantum Vacuum* (Academic Press, San Diego, 1994).
3. V. M. Mostepanenko and N. N. Trunov, *The Casimir Effect and its Applications* (Clarendon Press, Oxford, 1997).
4. M. Krech, *The Casimir Effect in Critical Systems* (World Scientific, Singapore, 1994).
5. K. A. Milton, *The Casimir Effect* (World Scientific, Singapore, 2001).
6. M. Kardar and R. Golestanian, *Rev. Mod. Phys.* **71**, 1233 (1999).
7. M. Bordag, U. Mohideen and V. M. Mostepanenko, *Phys. Rep.* **353**, 1 (2001).
8. S. K. Lamoreaux, *Rep. Progr. Phys.* **68**, 201 (2005).
9. S. K. Lamoreaux, *Phys. Rev. Lett.* **78**, 5 (1997).
10. U. Mohideen and A. Roy, *Phys. Rev. Lett.* **81**, 4549 (1998); G. L. Klimchitskaya, A. Roy, U. Mohideen and V. M. Mostepanenko, *Phys. Rev.* **A60**, 3487 (1999).
11. A. Roy and U. Mohideen, *Phys. Rev. Lett.* **82**, 4380 (1999).
12. A. Roy, C.-Y. Lin and U. Mohideen, *Phys. Rev.* **D60**, 111101(R) (1999).
13. B. W. Harris, F. Chen and U. Mohideen, *Phys. Rev.* **A62**, 052109 (2000); F. Chen, G. L. Klimchitskaya, U. Mohideen and V. M. Mostepanenko, *Phys. Rev.* **A69**, 022117 (2004).
14. T. Ederth, *Phys. Rev.* **A62**, 062104 (2000).
15. H. B. Chan, V. A. Aksyuk, R. N. Kleiman, D. J. Bishop and F. Capasso, *Science* **291**, 1941 (2001); *Phys. Rev. Lett.* **87**, 211801 (2001).
16. G. Bressi, G. Carugno, R. Onofrio and G. Ruoso, *Phys. Rev. Lett.* **88**, 041804 (2002).
17. F. Chen, U. Mohideen, G. L. Klimchitskaya and V. M. Mostepanenko, *Phys. Rev. Lett.* **88**, 101801 (2002); *Phys. Rev.* **A66**, 032113 (2002).
18. R. S. Decca, E. Fischbach, G. L. Klimchitskaya, D. E. Krause, D. López and V. M. Mostepanenko, *Phys. Rev.* **D68**, 116003 (2003).
19. R. S. Decca, D. López, E. Fischbach, G. L. Klimchitskaya, D. E. Krause and V. M. Mostepanenko, *Ann. Phys. (N.Y.)* **318**, 37 (2005).
20. G. L. Klimchitskaya, R. S. Decca, E. Fischbach, D. E. Krause, D. López and V. M. Mostepanenko, *Int. J. Mod. Phys.* **A20**, 2205 (2005).

21. F. Chen, U. Mohideen, G. L. Klimchitskaya and V. M. Mostepanenko, *Phys. Rev.* **A72**, 020101(R) (2005); **A74**, 022103 (2006).
22. F. Chen, G. L. Klimchitskaya, V. M. Mostepanenko and U. Mohideen, *Phys. Rev. Lett.* **97**, 170402 (2006).
23. F. Chen, G. L. Klimchitskaya, V. M. Mostepanenko and U. Mohideen, quant-ph/0610094.
24. T. Emig, R. L. Jaffe, M. Kardar and A. Scardicchio, *Phys. Rev. Lett.* **96**, 080403 (2006).
25. M. Bordag, *Phys. Rev.* **D73**, 125018 (2006).
26. V. B. Bezerra, R. S. Decca, E. Fischbach, B. Geyer, G. L. Klimchitskaya, D. E. Krause, D. López, V. M. Mostepanenko and C. Romero, *Phys. Rev.* **E73**, 028101 (2006).
27. J. S. Høye, I. Brevik, J. B. Aarseth and K. A. Milton, *J. Phys.* **A39**, 6031 (2006).
28. B. Geyer, G. L. Klimchitskaya and V. M. Mostepanenko, *Phys. Rev.* **D72**, 085009 (2005).
29. G. L. Klimchitskaya, B. Geyer and V. M. Mostepanenko, *J. Phys.* **A39**, 6495 (2006).
30. B. Geyer, G. L. Klimchitskaya and V. M. Mostepanenko, *Int. J. Mod. Phys.* **A21**, 5007 (2006).
31. R. S. Decca, D. López, H. B. Chan, E. Fischbach, D. E. Krause and C. R. Jamell, *Phys. Rev. Lett.* **94**, 240401 (2005).
32. A. Bulgac, P. Magierski and A. Wirzba, *Phys. Rev.* **D73**, 025007 (2006).
33. H. Gies and K. Klingmüller, *Phys. Rev. Lett.* **96**, 220401 (2006); *Phys. Rev.* **D74**, 045002 (2006).
34. V. B. Bezerra, G. L. Klimchitskaya, V. M. Mostepanenko, and C. Romero, *Phys. Rev.* **A69**, 022119 (2004).
35. V. M. Mostepanenko, V. B. Bezerra, R. S. Decca, E. Fischbach, B. Geyer, G. L. Klimchitskaya, D. E. Krause, D. López and C. Romero, *J. Phys.* **A39**, 6589 (2006).
36. E. M. Lifshitz and L. P. Pitaevskii, *Statistical Physics* Pt. II (Pergamon Press, Oxford, 1980).
37. J. Blocki, J. Randrup, W. J. Swiatecki and C. F. Tsang, *Ann. Phys. (N.Y.)* **105**, 427 (1977).
38. R. B. Rodrigues, P. A. Maia Neto, A. Lambrecht and S. Reynaud, *Phys. Rev. Lett.* **96**, 100402 (2006).
39. A. Lambrecht, P. A. Maia Neto and S. Reynaud, *New J. Phys.* **8**, 243 (2006).
40. F. Chen, U. Mohideen, G. L. Klimchitskaya and V. M. Mostepanenko, *Phys. Rev. Lett.* **98**, 068901 (2007).
41. R. B. Rodrigues, P. A. Maia Neto, A. Lambrecht and S. Reynaud, *Phys. Rev. Lett.* **98**, 068902 (2007).
42. T. Emig, A. Hanke, R. Golestanian and M. Kardar, *Phys. Rev. Lett.* **87**, 260402 (2001); *Phys. Rev.* **A67**, 022114 (2003).
43. R. Büscher and T. Emig, *Phys. Rev. Lett.* **94**, 133901 (2005).
44. *Handbook of Optical Constants of Solids*, ed. E. D. Palik (Academic Press, New York, 1985).
45. G. Bimonte, E. Calloni, G. Esposito, L. Milano and L. Rosa, *Phys. Rev. Lett.* **94**, 180402 (2005); G. Bimonte, E. Calloni, G. Esposito and L. Rosa, *Nucl. Phys.* **B726**, 441 (2005).
46. J. N. Munday, D. Iannuzzi, Y. Barash and F. Capasso, *Phys. Rev.* **A71**, 042102 (2005).
47. M. Brown-Hayes, D. A. R. Dalvit, F. D. Mazzitelli, W. J. Kim and R. Onofrio, *Phys. Rev.* **A72**, 052102 (2005).
48. P. Antonini, G. Bressi, G. Carugno, G. Galeazzi, G. Messineo and G. Ruoso, *New J. Phys.* **8**, 239 (2006).

49. S. K. Lamoreaux and W. T. Buttler, *Phys. Rev.* **E71**, 036109 (2005).
50. V. Petrov, M. Petrov, V. Bryksin, J. Petter and T. Tschudi, *Opt. Lett.* **31**, 3167 (2006).
51. J. Schwinger, L. L. DeRaad and K. A. Milton, *Ann. Phys. (N.Y.)* **115**, 1 (1978).
52. J. Feinberg, A. Mann and M. Revzen, *Ann. Phys. (N.Y.)*, **288**, 103 (2001).
53. A. Scardicchio and R. L. Jaffe, *Nucl. Phys.* **B743**, 249 (2006).
54. M. Boström and B. E. Sernelius, *Phys. Rev. Lett.* **84**, 4757 (2000).
55. J. S. Høye, I. Brevik, J. B. Aarseth and K. A. Milton, *Phys. Rev.* **E67**, 056116 (2003).
56. I. Brevik, J. B. Aarseth, J. S. Høye and K. A. Milton, *Phys. Rev.* **E71**, 056101 (2005).
57. I. Brevik, S. A. Ellingsen and K. A. Milton, *New J. Phys.* **8**, 236 (2006).
58. C. Genet, A. Lambrecht and S. Reynaud, *Phys. Rev.* **A62**, 012110 (2000).
59. M. Bordag, B. Geyer, G. L. Klimchitskaya and V. M. Mostepanenko, *Phys. Rev. Lett.* **85**, 503 (2000).
60. E. M. Lifshitz and L. P. Pitaevskii, *Physical Kinetics* (Pergamon Press, Oxford, 1980).
61. V. B. Bezerra, G. L. Klimchitskaya and C. Romero, *Phys. Rev.* **A65**, 012111 (2002).
62. B. Geyer, G. L. Klimchitskaya and V. M. Mostepanenko, *Phys. Rev.* **A67**, 062102 (2003).
63. V. B. Bezerra, G. L. Klimchitskaya and V. M. Mostepanenko, *Phys. Rev.* **A66**, 062112 (2002).
64. V. B. Bezerra, G. L. Klimchitskaya, V. M. Mostepanenko and C. Romero, *Phys. Rev.* **A69**, 022119 (2004).
65. M. Boström and B. E. Sernelius, *Physica* **A339**, 53 (2004).
66. B. E. Sernelius, *Phys. Rev.* **B71**, 235114 (2005); *J. Phys.* **A39**, 6741 (2006).
67. G. L. Klimchitskaya and V. M. Mostepanenko, *Phys. Rev.* **B75**, 036101 (2007).
68. V. M. Agranovich and V. L. Ginzburg, *Crystal Optics with Spatial Dispersion, and Excitons* (Springer, Berlin, 1984).
69. B. E. Sernelius, *Phys. Rev.* **B75**, 036102 (2007).
70. J. T. Foley and A. J. Devaney, *Phys. Rev.* **B12**, 3104 (1975).
71. G. L. Klimchitskaya and B. Geyer, These Proceedings.
72. F. Intravaia and A. Lambrecht, *Phys. Rev. Lett.* **94**, 110404 (2005).
73. M. Bordag, *J. Phys.* **A39**, 6173 (2006).
74. I. Pirozhenko, A. Lambrecht and V. B. Svetovoy, *New J. Phys.* **8**, 238 (2006).
75. A. Lambrecht and S. Reynaud, *Eur. Phys. J.* **D8**, 309 (2000).
76. S. G. Rabinovich, *Measurement Errors and Uncertainties* (Springer, New York, 2000).
77. R. S. Decca, private communication.
78. E. Fischbach and C. L. Talmadge, *The Search for Non-Newtonian Gravity* (Springer, New York, 1999).
79. S. Dimopoulos and G. F. Giudice, *Phys. Lett.* **B379**, 105 (1996).
80. I. Antoniadis, N. Arkani-Hamed, S. Dimopoulos and G. Dvali, *Phys. Lett.* **B436**, 257 (1998).
81. N. Arkani-Hamed, S. Dimopoulos and G. Dvali, *Phys. Rev.* **D59**, 086004 (1999).
82. M. Bordag, B. Geyer, G. L. Klimchitskaya and V. M. Mostepanenko, *Phys. Rev.* **D58**, 075003 (1998); **D60**, 055004 (1999); **D62**, 011701(R) (2000).
83. J. C. Long, H. W. Chan and J. C. Price, *Nucl. Phys.* **B539**, 23 (1999).
84. V. M. Mostepanenko and M. Novello, *Phys. Rev.* **D63**, 115003 (2001).
85. E. Fischbach, D. E. Krause, V. M. Mostepanenko and M. Novello, *Phys. Rev.* **D64**, 075010 (2001).
86. S. J. Smullin, A. A. Geraci, D. M. Weld, J. Chiaverini, S. Holmes and A. Kapitulnik, *Phys. Rev.* **D72**, 122001 (2005).
87. D.J. Kapner, T. S. Cook, E. G. Adelberger, J. H. Gundlach, B. R. Heckel, C. D. Hoyle and H. E. Swanson, *Phys. Rev. Lett.* **98**, 021101 (2007).